Chemical Physics xxx (2010) xxx–xxx

Contents lists available at ScienceDirect

Chemical Physics

journal homepage: www.elsevier.com/locate/chemphys

Extension of stochastic resonance in the dynamics of ice ages

Peter D. Ditlevsen

Centre for Ice and Climate, The Niels Bohr Institute, University of Copenhagen, Juliane Maries Vej 30, DK-2100 Copenhagen O, Denmark

ARTICLE INFO

Article history:
Available online xxxx

Keywords:
Stochastic resonance
Bifurcation structure
Ice ages

ABSTRACT

Understanding the dynamics of ice ages has been a major challenge in climate research for more than a century. The cycles are thus attributed to the climatic response of the orbital changes in the incoming solar radiation to the Earth. However, these changes in the forcing are too small to explain the observed climate variations as simple linear responses, thus non-linear amplifications of the orbital forcing are necessary to account for the glacial cycles. Stochastic resonance was proposed by Benzi et al. [1] to describe this scenario. However, there are several shortcomings in the description of the glacial cycles as a simple stochastic resonance. In order to account for the non-periodic nature of the ice age cycles, especially the shift 1 million years ago from 41-kyr ice age cycles to the present approximately 100-kyr ice age cycles, a non-trivial extension of the notion of a stochastic resonance is needed.

1. Introduction

The phenomenon of stochastic resonance has been observed in very many different physical systems [7]. It has its origin in the attempt of explaining the apparent amplification of small periodic changes in the insolation (INcomming SOLar radiATION) to the Earth into dramatic changes in climate through the glacial cycles. The cyclic repetition of glaciations are well documented through the last few million years by ocean sedimentation and other geological records. The apparent regularity of the glacial cycles early led to the proposal of an astronomic origin of the cause. These changes in insolation are referred to as the orbital forcing of the climate. The origin is the perturbation of Earths Keplerian orbit by the other planets and the Moon. It results in highly non-trivial changes in the insolation with latitude and time of year. The dominant orbital periods in insolation is the 41-kyr obliquity cycle (tilt of rotational axis, determining the meridional gradient in insolation) and the precessional cycles (determining the season when Earth is closest to the sun) which decompose into 19 kyr and 23 kyr periods. However, through the last 800 kyr – 1 Myr the dominant period for the glacial cycles is approximately 100-kyr similar to the one order of magnitude weaker eccentricity cycle (determining the semi-annual difference in distance to the sun). The weakness of this climatic forcing is referred to as the 100-kyr problem of the Milankovitch theory [15]. In the Plio- and early Pleistocene, 3–1 Myr BP (Before Present), the dominant period of variation was indeed the 41-kyr obliquity variation. The original stochastic resonance hypothesis of amplification of the eccentricity cycles should thus be revised. Combined evidence from records of glaciations on land and deep sea records suggest that the climate has shifted between different quasi-stable states characterized by the mode of the global ocean circulation and the degree of glaciation [14]. By comparison between the paleoclimatic record and the non-linear stochastic model, it is demonstrated that the record can be generated by the forcing from insolation changes due to the obliquity cycle through the full record including the last 1 Myr. The assumption here is that the orbital forcing resulted in periodic jumps between two stable climate states. What happened approximately 800 kyr – 1 Myr ago was that a third deep glacial state became accessible resulting in a change in length of the glacial cycles. The reason for this mid-Pleistocene transition (MPT) is unknown, and attributed to a gradual cooling due to a decreasing atmospheric CO_2 level [20] or a change in the bedrock erosion (the regolith hypothesis) [5].

Before presenting the new ice age model a short review of the geophysical basis for the classical stochastic resonance model of ice ages is given.

2. The energy balance

The stochastic resonance model is based on the assumption of a noise induced variations in a bistable climate with a periodic forcing by changing insolation due to changes in Earths orbit around the sun: The two states of glacial – and interglacial climates can be described through a simple 0-dimensional model of the global energy balance [2,21]. Defining T as the global average surface temperature, the change of the temperature T is determined by the difference in incoming and outgoing radiation [2,21]:

$$c\frac{dT}{dt} = R_i - R_o = (1-\alpha(T))S(\mu) - \sigma(T-\Delta T)^4, \quad (1)$$

E-mail address: pditlev@gfy.ku.dk

0301-0104/$ - see front matter © 2010 Elsevier B.V. All rights reserved.
doi:10.1016/j.chemphys.2010.05.022

where c is the heat capacity, $S(\mu) = S^*/4$ is a quarter of the solar constant. (The quarter comes from the ratio of the surface of the sphere to the cross-sectional area blocking the sun light). The parameter μ indicates that the insolation is a function of Earth's changing orbital parameters. $T_{eff} = T - \Delta T$ is the temperature at the level in the atmosphere from where the black body radiation is emitted to space. Since the atmosphere is opaque in the infra-red wave-band due to greenhouse gas absorbers this level is estimated as one optical depth into the atmosphere in this band. The greenhouse effect, the change in cloudiness and other factors must all be expressed through the temperature difference ΔT, which is itself some non-linear function of T, here modeled following [21].

The albedo $\alpha(T)$ is the fraction of the sunlight hitting the planet which is reflected back into space. The planetary albedo is not a constant factor, it depends, through the amount of clouds and ice, on the state of the climate itself.

The amount of ice and snow is larger when the temperature is lower, so the lower the temperature the higher albedo, and we can write the albedo $\alpha(T)$ as $\alpha(T) = \alpha_1 1\mathrm{I}_{(T\leqslant T_1)} + ((T_2 - T)\alpha_1 + (T - T_1)\alpha_2)/(T_2 - T_1)1\mathrm{I}_{(T_1<T\leqslant T_2)} + \alpha_2 1\mathrm{I}_{(T>T_2)}$, where $1I_I$ is the indicator function for the interval I. If the temperature is below some low temperature T_1 the planet will be completely ice covered and a further decrease in temperature cannot increase the albedo. If the temperature is above some other high temperature T_2 the ice is completely melted and a further increase in temperature will not lead to a decrease in albedo. In between we use a simple linear interpolation.

The behavior of (1) is easily understood from a graphic representation. Fig. 1A shows the incoming and outgoing radiation as a function of temperature. There are three temperatures T_a, T_b, T_c for which the curves cross such that the incoming – and outgoing radiations are in balance. These points are the fixed points of (1). Consider the climate to be at point T_a. If some small perturbation makes the temperature lower than T_a we will have $R_i > R_o \Rightarrow cdT/dt > 0$ and the temperature will rise to T_a. If on the other hand the perturbation is positive and the temperature is a small amount larger than T_a we have $R_i > R_o \Rightarrow cdT/dt > 0$ and the temperature will decrease to T_a again. Thus T_a is a stable fixed point. The same analysis shows that T_b is an unstable and T_c is a stable fixed point.

A convenient way of writing Eq. (1) is in terms of a potential $U(x, \mu)$:

$$\frac{dT}{dt} = -\partial_T U(T, \mu), \tag{2}$$

where from (1) we get $U(T, \mu) = -\int^T (R_i(\mu) - R_o)dT/c$. The potential is shown in Fig. 1B. The red curves in panels A and B indicate the change resulting from changing the insolation. For large enough change one of the stable and the unstable fixed points merge and disappears, the system undergoes a saddle node bifurcation. Fig. 1C shows the steady states as functions of the control parameter μ. This is the bifurcation diagram of the dynamical system in Eq. (1).

If the periodic changes in the control parameter is such that the two bifurcation points (b_1 and b_2) are not reached, transitions could only occur from noise induced fluctuations. The effect of all other dynamical variables of the system on the one effective variable T is modeled as a noise: $dT = -\partial_T U(T, \mu)dt + \sigma dB$, where dB is a Gaussian white noise with $dB^2 = dt$ and σ is the intensity of the noise. If furthermore the orbital forcing is assumed to show a simple sinusoidal variation, $S(\mu)(1 - \alpha) = S(0)(1 - \alpha) + A\sin\mu(t)$, with $\mu(t) = \omega t$, the governing equation becomes:

$$dT = -\partial_T U(T, 0) + A\sin\omega t + \sigma dB. \tag{3}$$

This is the typical model of stochastic resonance. A realization with σ tuned to the resonance is shown in Fig. 1D.

The present climate is the climate state T_c where the ice albedo does not play a significant role in cooling the Earth. However, the glacial climate does not correspond to the climate state T_a, since this is a completely ice covered planet. This climate state rather corresponds to the Snowball Earth, which seems to have occurred a few times some 700 million years ago [9]. The way out of the Snowball Earth is thought to be a steady increase in greenhouse gasses from volcanism increasing ΔT driving the system to the bifurcation point b_1 in Fig. 1C.

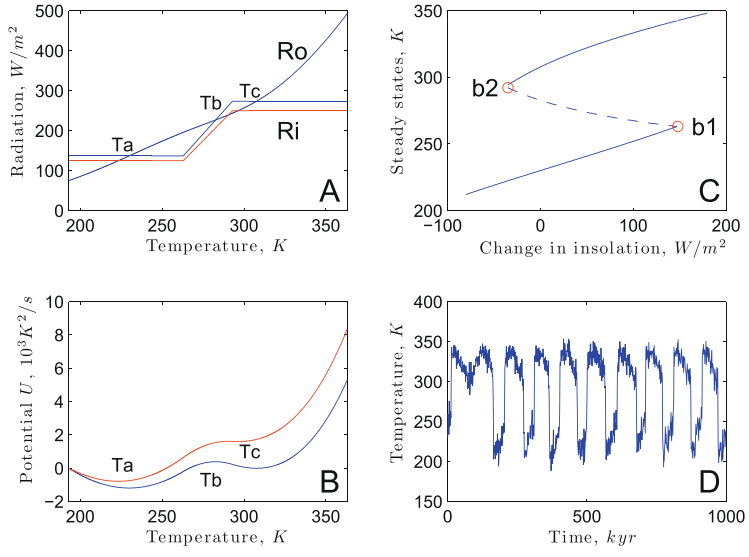

Fig. 1. The stochastic resonance model of ice ages. Panel A shows the balance between the incoming short wave solar radiation R_i and the outgoing long wave radiation R_o as functions of global mean surface temperature. Where the curves cross the in- and out going radiation balance and the temperature does not change. The red curve is the incoming radiation for a situation where Earth's orbit results in reduced insolation. Panel B shows the potential corresponding to the forcing $R_i - R_o$ in Panel A in the two cases. Panel C shows the bifurcation diagram for the energy balance model. Note that the bifurcation point b_2 is almost reached in case of the red curves in Panels A and B. Panel D shows a realization of the stochastic resonance Eq. (3). (For interpretation of the references to colour in this figure legend, the reader is referred to the web version of this article.)

Please cite this article in press as: P.D. Ditlevsen, Chem. Phys. (2010), doi:10.1016/j.chemphys.2010.05.022

3. The effective dynamics

It has been demonstrated that high dimensional ocean models [18] have a structure of stability and bifurcation points similar to low dimensional models as the energy balance model described above. In this case, the effective variable is the total meridional overturning in the Atlantic ocean. It is thus plausible that within the high dimensional climate system there are slow manifolds for which bifurcation points exist [4].

The first step is thus to identify the bifurcation structure of the climate system: Three quasi-stationary states have been proposed: G (deep glacial), g (pre-glacial), and i (interglacial), respectively [17]. The paleoclimatic record seems to indicate that certain transitions between the three states are forbidden. In the period 2–1 Myr BP the record shows regular oscillations between only the two states i and g, while in the period 1–0 Myr BP there is only a specific sequence of occurrences: $i \to g \to G \to i$ permitted. This observation constraints the possible bifurcation structure.

The climate dynamics is assumed reflected in a single variable $x(t)$. This is taken to be (minus) the global ice volume, represented by the deep sea oxygen isotope ratio, roughly proportional to global mean surface temperature anomaly. The dynamics is described by an effective non-linear stochastic differential equation,

$$dx = f_\alpha(x,\mu)dt + \sigma dB, \tag{4}$$

where the Gaussian white noise term dB with intensity σ again describes the influence of the non-resolved variables and the internally generated chaotic climate fluctuations. It is within this framework in which the roles of the orbital forcing and internal stochastic forcing is investigated. The deterministic part, $f_\alpha(x,\mu)$, of the dynamics depends on the external orbital forcing, labelled by a single control parameter μ and internal parameters, represented by α.

The full climate dynamics can obviously not be completely reconstructed by such a single valued function. However, since bifurcations describe the topology of the phase space, in higher dimensional realistic models, resolving more of the dynamics, the bifurcation structure should be unchanged and the dynamics thus robust with respect to the detailed dynamics modeled. It is thus the bifurcation structure of $f_\alpha(x,\mu)$, with respect to the control parameter μ, which determines the climate development.

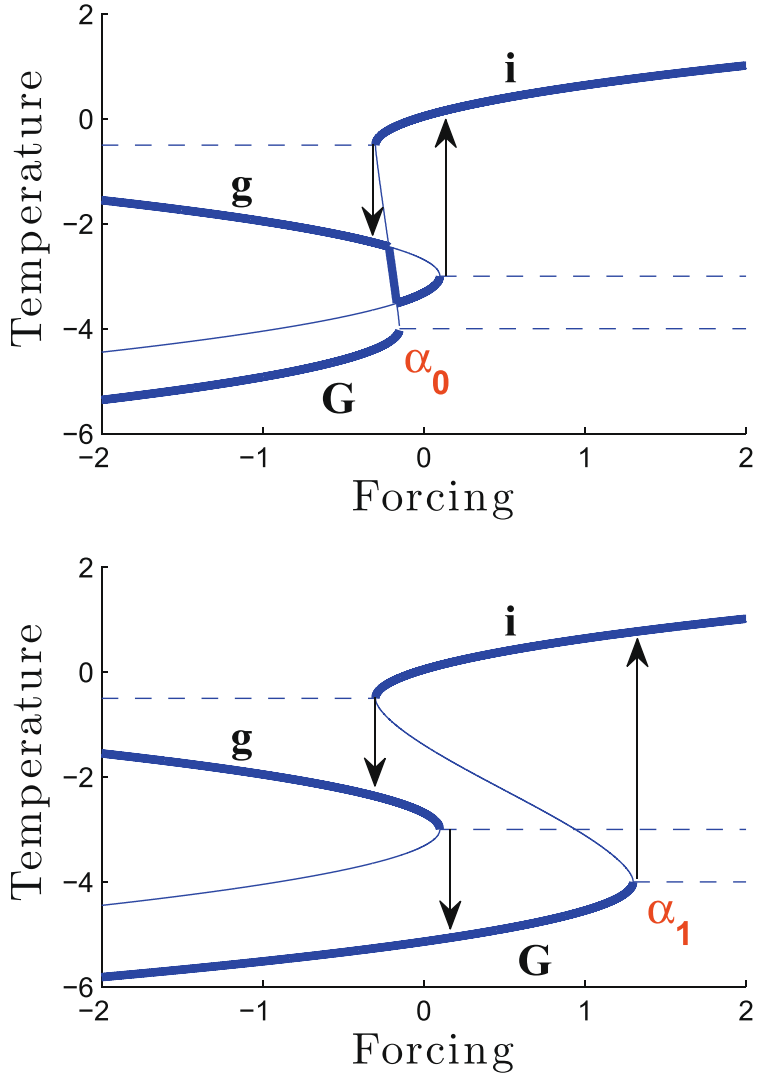

Fig. 2. The bifurcation diagram for the ice age model. Along the x-axis is the forcing represented by the control parameter μ, along the y-axis are the fixed points $\{x_0(\mu)|f(x_0,\mu)=0\}$ of the drift function $f_\alpha(x,\mu)$. The drift function is simply approximated by a fifth order polynomial, with the roots determined by the fixed points. The horizontal dashed line-segments indicates (real part of) sets of complex conjugate roots. The fat curves show the stable fixed points. The bifurcation point α is the point where the deep glacial state G disappears. The arrows indicate the hysteresis loop as the forcing parameter is changed. Upper panel: The glacial state G is not accessible. Lower panel: Now the location of the bifurcation point α has changed in such a way that the deep glacial state G is accessible.

Please cite this article in press as: P.D. Ditlevsen, Chem. Phys. (2010), doi:10.1016/j.chemphys.2010.05.022

Guided by the observed record and the transition rules we can construct an empirical bifurcation diagram: Fig. 2, upper panel, shows the bifurcation diagram for the drift function $f_\alpha(x,\mu)$ as a function of μ at the time interval 2–1 Myr BP. The bifurcation diagram shows the curves $\{x_0(\mu)|f(x_0,\mu)=0\}$. The fat curves are the stable fixed point curves for which $\partial_x f<0$, while the thin curves are the unstable fixed point curves for which $\partial_x f>0$. Thus in the case of no additional noise ($\sigma=0$) the state of the system $x(t)$ is uniquely determined from the initial state $x(0)$ and the development of the forcing $\mu(t)$.

In the real climate system the internal noise is substantial and the system will not reside exactly in the steady states determined by the bifurcation diagram. Thus the full drift function needs to be parametrized. The simplest way to parameterize the drift function in accordance with the bifurcation diagram is as a fifth order polynomial:

$$f_\alpha(x,\mu)=\prod_{j=1}^{5}(x-x_\alpha^j(\mu)), \tag{5}$$

where $x_\alpha^j(\mu)$ is the jth steady state (zero-points) in the bifurcation diagram. As labelled in the figure the parameter α determines the position of the lower bifurcation point. For more details see [6].

It should be noted that this is, of course, not the only possible drift function corresponding to this bifurcation diagram. In order to reconstruct the drift function from the observed realization, one could in principle obtain the stationary probability density $p_{\mu_0}(x)$ by sorting $x(t)$ according to $\mu(t)=\mu_0$. Assuming that $\mu(t)$ is changing slowly in comparison to the time scale for $x(t)$ to drift to a stationary state $x_0(f_\alpha(x_0,\mu)=0)$, one could then obtain $f_\alpha(x_0,\mu)$ by solving the Fokker–Planck equation [8] associated with Eq. (4) for fixed $\mu=\mu_0$. This would require a very long data series and complete absence of additional non-climatic noise in the proxy data. This is not the case for the existing paleoclimatic record.

4. The orbital forcing

For a model defined by Eq. (4) where the climate is characterized by one number, the global mean temperature, there is ambiguity in ascribing the orbital forcing from the time and space varying insolation field across the globe.

It has been argued already by Milankovitch [16] that the summer insolation around the southern rim of the large glacial ice sheets in the northern hemisphere governs the melting of the ice, thus the dominant component of the orbital forcing (called the Milankovitch forcing) is defined as the summer solstice insolation at 65 N latitude. This forcing is strongly dominated by the approximately 20-kyr precessional cycle, which is not strong in the climatic record. What is relevant for melting of the glaciers is rather the insolation during the summer period where temperatures are above freezing. Thus another measure of the orbital forcing would be the insolation integrated over the period with melting, termed the degree days. Here we shall assume the integrated insolation exceeding 200 W/m^2 to be a proxy for the degree days forcing. This measure is dominated by the obliquity cycle

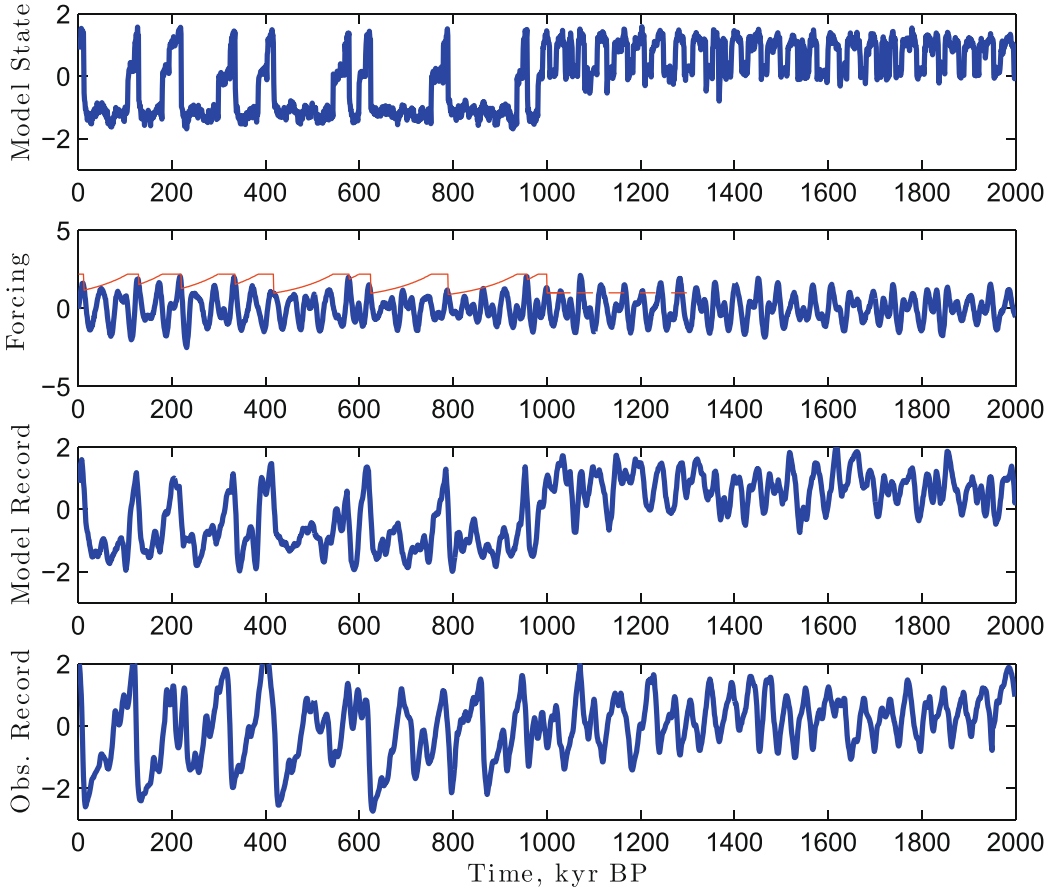

Fig. 3. The top panel shows a realization of the model. Second panel shows the orbital forcing driving the model. The red curve shows $\alpha(t)$, where the jumps to $\alpha=\alpha_1$ are triggered by the transition $G\to i$. The next transition is in the low noise limit only possible when the blue curve is above the red curve. The third panel shows a "pseudo paleorecord", where a red noise component representing the non-climatic noise, is added to the model realization in the top panel. Lower panel shows the (normalized) paleoclimatic isotope record from a composite of ocean cores. The record is a proxy for the global sea level or minus the global ice volume. See text for more explanations. (For interpretation of the references to colour in this figure legend, the reader is referred to the web version of this article.)

Please cite this article in press as: P.D. Ditlevsen, Chem. Phys. (2010), doi:10.1016/j.chemphys.2010.05.022

since the increased insolation when Earth is close to the sun in its orbit is compensated by shorter time spend there due to Kepler's second law [12,13]. Thus the total insolation during the degree days becomes independent of the precessional cycle.

The two proposed forcings (degree day insolation and summer solstice insolation) are different, since the latter has a strong component of the precessional cycle. Using the summer solstice insolation as the better proxy for the forcing can be rationalized from the point of view of a threshold crossing dynamics, since the extremal values would then be the governing parameter. Using the degree day insolation can be rationalized from assuming the summer melting of ice to be the governing climatic driver. Since we cannot decide between the two within the framework of a simple model, we shall take the alternative approach of assuming the linear combination of the two, considered as a first order expansion, which gives the best fit between the observed record as response to the forcing. Thus the forcing is taken to be a linear combination of the summer solstice 65 N insolation (f_{ss}) and the integrated summer insolation at 65 N ($\bar{f}_I$), where the summer period is defined as the period where the daily mean insolation exceeds $I = 200$ W/m^2.

The model results presented in the following are robust with respect to the threshold I chosen in a rather broad interval. The forcing, $f = \lambda \bar{f}_I + (1-\lambda) f_{ss}$, shown in Fig. 3, second panel, is calculated using the code provided by Eisenman and Huybers [11]. Values of λ around 0.5 gives the best result, $\lambda = 0.5$ is used. The f_{ss} component has a relatively strong precessional component which is absent in $\bar{f}_I$. For small values of λ there is an overwhelming probability of the last glacial termination to occur 41-kyr prior to what is observed. Thus the assignment $\lambda \approx 0.5$ might, within the framework of the non-linear model, be interpreted as an empirical determination of the dominating components of the orbital forcing.

5. The hysteresis behavior

The diagram in Fig. 2, upper panel, shows the fixed points of $f_\alpha(x,\mu)$ as a function of the deterministic forcing μ. The three branches of stable fixed points $x^i(\mu)$ for the function, such that $f_\alpha(x^i,\mu) = 0$ and $\partial_x f_\alpha(x^i,\mu) < 0$, are indicated by fat curves. The specification of the $x^i(\mu)$'s and Eqs. (1) and (2) completely defines the model. Since x is a proxy for global mean surface temperature anomaly (or minus global ice volume), the lower branch corresponds to the deep glacial state G. The middle branch corresponds to the climate state g and the upper branch to the interglacial state i. The thin curves correspond to the separating unstable fixed points. The dashed line-segments correspond to pairs of complex conjugate roots in the fifth order polynomial. Note again that assuming a polynomial drift function, this is uniquely determined from the roots, except from a trivial multiplicative constant.

Suppose now that the climate is in either of the states g or i and the climatic noise is too weak to induce a crossing of a barrier separating the stable states. Then the only way a forcing induced shift between the climate states can occur is through bifurcations and a hysteresis as sketched by the arrows. Clearly the climate state G can only be reached by a noise induced transition.

Assume now that the lower bifurcation point, indicated by α_0 in Fig. 2, upper panel, moves toward larger values of μ indicating that

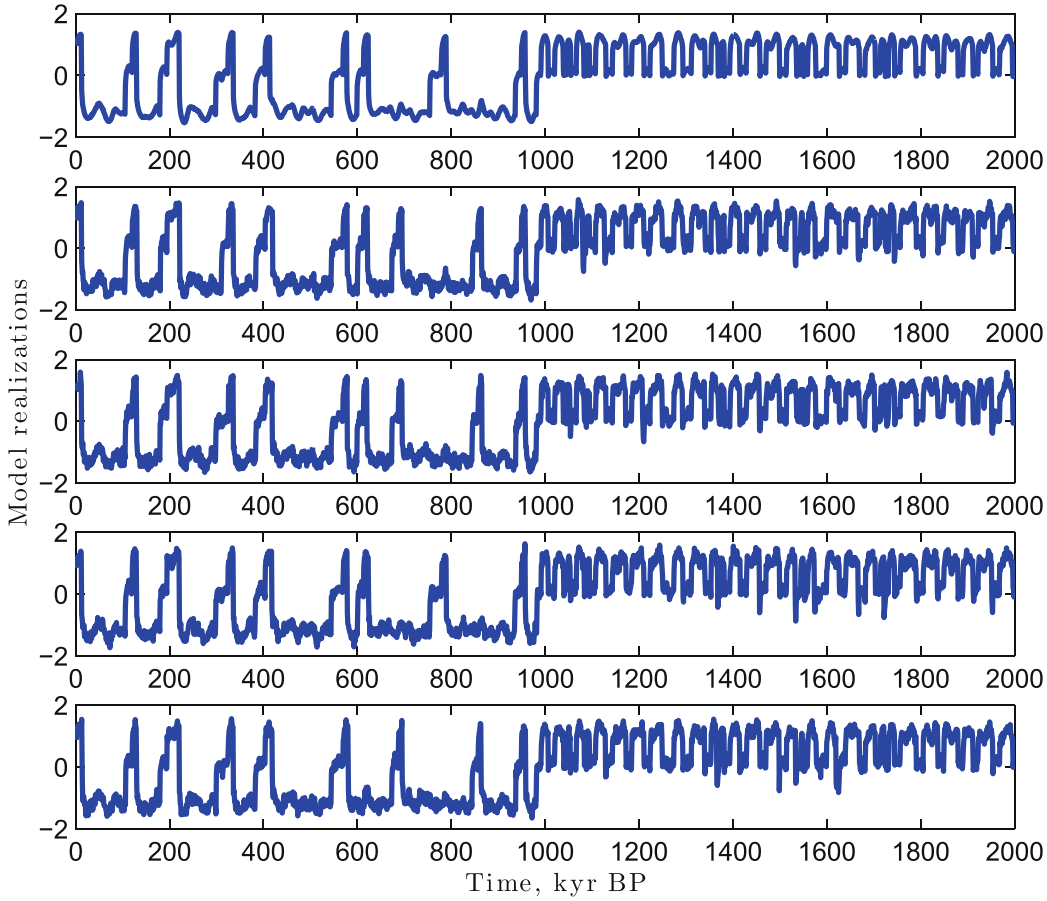

Fig. 4. Five realizations of the model with the same orbital forcing and different stochastic forcing. The first panel shows a realization without stochastic forcing. This is the purely deterministic climate response to the orbital forcing. The bottom four realizations has a noise intensity $\sigma = 0.8$ K/$\sqrt{\text{kyr}}$. It is seen that only in the last part of the 100-kyr world the timing of the terminations are independent from the noise. In all five realizations an additional non-climatic "proxy noise" is added aposterior.

Please cite this article in press as: P.D. Ditlevsen, Chem. Phys. (2010), doi:10.1016/j.chemphys.2010.05.022

a stronger forcing is needed in order to destabilize the deep glacial state. In this case, $\alpha_0 \to \alpha_1$ shown in Fig. 2, lower panel, the glacial state G is now reachable and a hysteresis loop $i \to g \to G \to i$ will appear. The central postulate of the model is the change in this bifurcation structure represented by the shift of the point α (from α_0 to α_1 on the μ-axis) at the Mid-Pleistocene transition.

The change in the position of the lower bifurcation point is modeled such that $\alpha = \alpha_1$ when the climate is in state i. When the state G is reached through two bifurcations, α is gradually changing. The gradual change in the bifurcation diagram is modeled as a relaxation, $d\alpha/dt = -(\alpha - \alpha_0)/\tau$, where α_0 is the early Pleistocene equilibrium value and τ is a relaxation time. When the climate bifurcates through the rapid transition $G \to i$, the parameter α again change to α_1.

In order for the climate to skip the 41-kyr obliquity pacing of deglaciations the timescale τ governing the bifurcation structure must be considerably longer than 41-kyr. The model results are quite insensitive to the specific value of τ in the interval 70–130 kyr, and is set to be 100-kyr. This is very long time scale even compared to buildup of the large ice sheets. The origin of the physical processes related to this time scale are unknown. Obvious candidates are erotion processes in the lithosphere and the geo-chemical carbon-CO_2 cycles.

6. Comparison between the paleoclimatic record and the model

Fig. 3, first panel, shows a particular realization of the model. The second panel shows the forcing, the red curve shows the value of α, which is defined as the position of the lower bifurcation point in Fig. 2 along the axis of the forcing (the x-axis). Note that a transition $G \to i$ without noise assistance is only possible when the forcing exceeds the value of alpha (that is when the blue curve is above the red curve in the second panel).

The composite Atlantic ocean sedimentation record for the period 0–2000 kyr BP is shown in the bottom panel [10]. The record is the benthic oxygen isotope sequence. The curve is plotted with normalized variance and the mean subtracted. This is a proxy for the global ice volume. The dating is based on a depth-age model independent from astronomical tuning.

The differences between the single records compositing the stacked record gives an estimate of the additional noise from bioturbation and other factors that makes the record different from a true record of ice volume. So in order to compare the model with the observed climate record an additional red noise, of the same magnitude as the difference in deep sea records is added to the model. This is shown in the third panel, which should be compared with the observed record in fourth panel.

7. The role of the stochastic noise

In order to investigate the role of the stochastic noise a set of realizations of the model are presented in Fig. 4. For the comparison between the model and the proxy climate records we focus on the rapid transitions $G \to i$, called terminations [3,19]. The top panel shows a realization with no stochastic noise. This is the deterministic climate response to the orbital forcing. It is seen that the last five terminations are reproduced as observed, but there are fewer interglacials in the earlier part of the late-Pleisocene period (1000–500 kyr BP) than in the observed record. From Fig. 3, second panel, it is seen that the amplitude of the orbital forcing is low in this period. The bottom four panels show different realizations with a moderate stochastic forcing ($\sigma = 0.8\ \mathrm{K}/\sqrt{\mathrm{kyr}}$). In these realizations the added noise induces additional terminations at different times, suggesting a fundamental unpredictability in glacial terminations. With a larger intensity stochastic forcing the terminations tend to occur at more obliquity cycles, corresponding to 41-kyr ice ages, contrary to the observations for the late Pleistocene record. This compares well with the observed record (Fig. 3, lower panel) where the marine isotope stage 7 (approx. 250–200 kyr BP) seems to be split into two periods.

Even though the observed ice age history is not expected to be reproduced in a given model realization, the spectral density is similar. The spectral signature of the change in the climatic record from the 41-kyr world (2–1 Myr BP) to the 100-kyr world (1–0 Myr

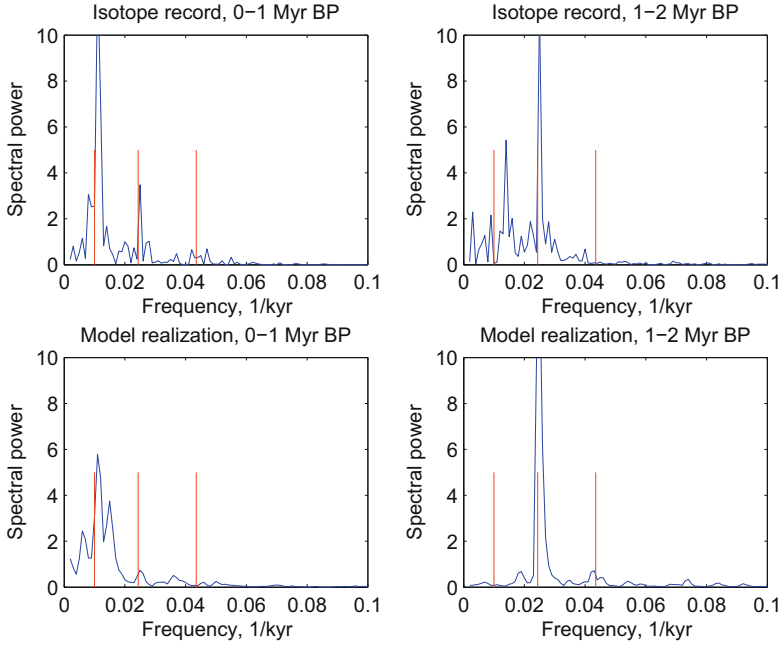

Fig. 5. Upper panel: The spectral power of the sediment records for the two periods, 0–1 Myr and 1–2 Myr. The red markers indicate 100-kyr, 41-kyr and 23-kyr periods. The lower panels show the corresponding spectra for the randomly chosen realization of the model shown in Fig. 4. Both the climate record and the model show a transition from the '41-kyr world' to the '100-kyr world'. (For interpretation of the references to colour in this figure legend, the reader is referred to the web version of this article.)

Please cite this article in press as: P.D. Ditlevsen, Chem. Phys. (2010), doi:10.1016/j.chemphys.2010.05.022

BP) is shown in Fig. 5. The spectral signature is well reproduced in the randomly chosen model realization.

8. Summary

In summary the empirical stochastic model presented support the suggestion that the transition from the '41-kyr world' to the '100-kyr world' occurring approximately 1 Myr – 800 kyr BP is due to a structural change in the bifurcation diagram describing the stability of the system as a function of the forcing. The glacial cycles are not solely a deterministic response to the orbital cycles. The internal noise also plays a role in triggering the jumps between the different climatic states in the first part of the '100-kyr world', in this period the apparently regular periodic occurrence of ice ages is driven by the noise. Had the noise component been larger, the ice ages would last for 41 kyrs, had it been smaller the climate would stay in the deep glacial state for very long. In this sense the early 100-kyr world is governed by a (generalized) stochastic resonance. Currently the state-of-the-art general circulation climate models are far from being able to simulate the observed glacial climate variations. It is even not known if they possess a non-trivial bifurcation structure.

References

[1] R. Benzi, G. Parisi, A. Sutera, A. Vulpiani, Tellus 34 (1982) 10.
[2] M.I. Bodyko, Tellus 21 (1969) 611.
[3] S.W. Broecker, Terminations, in: A. Berger, J. Imbrie, J. Hays, G. Kukla, B. Saltzman (Eds.), Milankovitch and Climate: Understanding the Response to Astronomical Forcing, D. Reidel Publishing Company, Dordrecht-Holland, 1984, p. 687.
[4] W.S. Broecker, Science 278 (1997) 1582.
[5] P.U. Clark, D. Pollard, Paleoceanography 13 (1998) 1.
[6] P.D. Ditlevsen, Paleoceanography 24 (2009) PA3204.
[7] L. Gammaitoni, P. Hanggi, P. Jung, F. Marchesoni, Rev. Mod. Phys. 70 (1998) 223.
[8] C.W. Gardiner, Handbook of Stochastic Methods, Springer Verlag, NY, 1985.
[9] P.F. Hoffman, A.J. Kaufman, G.P. Halverson, D.P. Schrag, Science 281 (1998) 1342.
[10] P. Huybers, Quat. Sci. Rev. 26 (2007) 37.
[11] P. Huybers, I. Eisenman, Integrated summer insolation calculations, NOAA/NCDC Paleoclimatology Program, Data Contribution # 2006-079, 2006, <http://www.ncdc.noaa.gov/paleo/forcing.html>.
[12] P. Huybers, E. Tziperman, Paleoceanography 23 (2008) PAI208.
[13] P. Huybers, C. Wunsch, Nature 434 (2005) 491.
[14] J. Imbrie, E.A. Boyle, S.C. Clemens, A. Duffy, W.R. Howard, G. Kukla, J. Kutzbach, D.G. Martinson, A. McIntyre, A.C. Mix, B. Molfino, J.J. Morley, L.C. Peterson, N.G. Pisias, W.L. Prell, M.E. Raymo, N.J. Shackleton, J.R. Toggweiler, Paleoceanlography 7 (1992) 701.
[15] J. Imbrie et al., Paleoceanography 8 (1993) 699.
[16] M. Milankovitch, Mathematiche Klimalehre und Astronomiche Theorie der Klimaschwankungen, Handbuch der Klimalogie Band 1 Teil A. Borntrager, Berlin, 1930.
[17] D. Paillard, Nature 391 (1998) 378.
[18] S. Rahmstorf, Nature 378 (1995) 145.
[19] M.E. Raymo, Paleoceanography 12 (1997) 577.
[20] B. Saltzman, K.A. Maasch, Clim. Dyn. 5 (1991) 201.
[21] W.D. Sellers, A global climatic model based on the energy balance of the earth-atmosphere system, J. Appl. Meteorol. 8 (1969) 392.

Please cite this article in press as: P.D. Ditlevsen, Chem. Phys. (2010), doi:10.1016/j.chemphys.2010.05.022